

Ion trapping techniques

S. Renuka Prasad*, Partha Pratim Datta and A. G. Menon

Department of Instrumentation, Indian Institute of Science, Bangalore 560 012, India

*Present address: LOGICS, 968, 2nd Main, 3rd Cross, Vijayanagar, Bangalore 560 040, India

Ion traps are widely used in optical spectroscopy, metrology and mass spectrometry. Targeted ions (formed either *in situ* or transported into the trap from an external source) are isolated and trapped using magnetic and/or electric fields. Over the past 15 years several different trap designs have emerged for different applications. All these designs are variants of one of the three generic traps – the Penning trap, the linear trap and the Paul trap. This paper will outline the method used to trap ions by these three techniques.

ION traps are devices which use magnetic and/or electric fields to confine the ions in a small region of space to carry out a variety of studies ranging from measurement of optical spectroscopic properties of an isolated single ion to mass spectrometric studies of an ensemble of fragment ions. Techniques for trapping ions vary markedly both in their principle of operation as also in the complexity of implementation. In literature numerous variants of three basic designs have been reported. These are (a) Penning¹ trap, where trapping is achieved by using a quadrupolar electric field and an axial magnetic field (b) linear traps², which use two-dimensional *rf* quadrupole fields and (c) Paul traps³ which uses three-dimensional quadrupolar field to trap ions.

This brief overview has the motivation of introducing a few basic concepts specific to each of these three techniques. This paper is not a review of current research in the area of ion traps but it is instead an effort to collate and present information required for understanding the criticalities of each technique. The topics chosen to be highlighted and the manner of presentation will certainly suffer from biases of our perspective but a study of references cited will rectify this shortcoming.

Penning trap

Ion motion

Penning traps are devices that use both magnetic field as well as electric field to trap ions. The shape of the trap used by mass spectroscopists varies considerably, from a simple cubic design to multicell and segmented design to facilitate tandem experiments⁴. Optical spectroscopists, on the other hand, have quite uniformly relied

on the three electrode geometry⁵ (similar to that used in the Paul trap, to be discussed later), to produce a quadrupolar field for trapping ions. While the magnetic field is used to restrict excursion of the ions in the radial direction, low voltage dc potential on the end-cap electrodes trap ions in the axial direction (Figure 1).

Ions in a uniform electric and magnetic field experience the Lorentz force, \vec{F} , given by⁶

$$\vec{F} = m \frac{d\vec{v}}{dt} = q\vec{E} + q\vec{v} \times \vec{B}, \quad (1)$$

where \vec{E} , \vec{v} and \vec{B} are the electric field, velocity, magnetic field vectors and q is the charge of the ion of mass m . In the absence of an electric field, the force on the ion is the vector cross product of the velocity and magnetic field, or

$$m \frac{d\vec{v}}{dt} = q\vec{v} \times \vec{B}. \quad (2)$$

From this equation it is possible to derive the cyclotron frequency ω_c as⁶

$$\omega_c = 2\pi\nu_c = q \frac{B_0}{m}, \quad (3)$$

where B_0 is the static magnetic field. Ions within the cell are trapped by the magnetic field in a plane perpendicular to the magnetic field but are free to move along the direction of the magnetic field. In view of this, it becomes necessary to apply a small dc bias potential on the two electrodes that are perpendicular to magnetic field axis. This dc potential creates a field that will now have to be incorporated to eq. (1). For a cubic cell with an assumed quadratically varying potential between the trapping electrodes, the field in the radial direction may be represented as⁶,

$$E(r) = E_0 r, \quad (4)$$

where $E_0 = 2\alpha V_z/a^2$ and $\alpha = 1.386$, a is the cell dimension, V_z is the trapping potential and r is the distance in the radial (x, y) direction from the centre. This radial field has the effect of producing a force in the outward direction, which is opposed, by the inward-directed

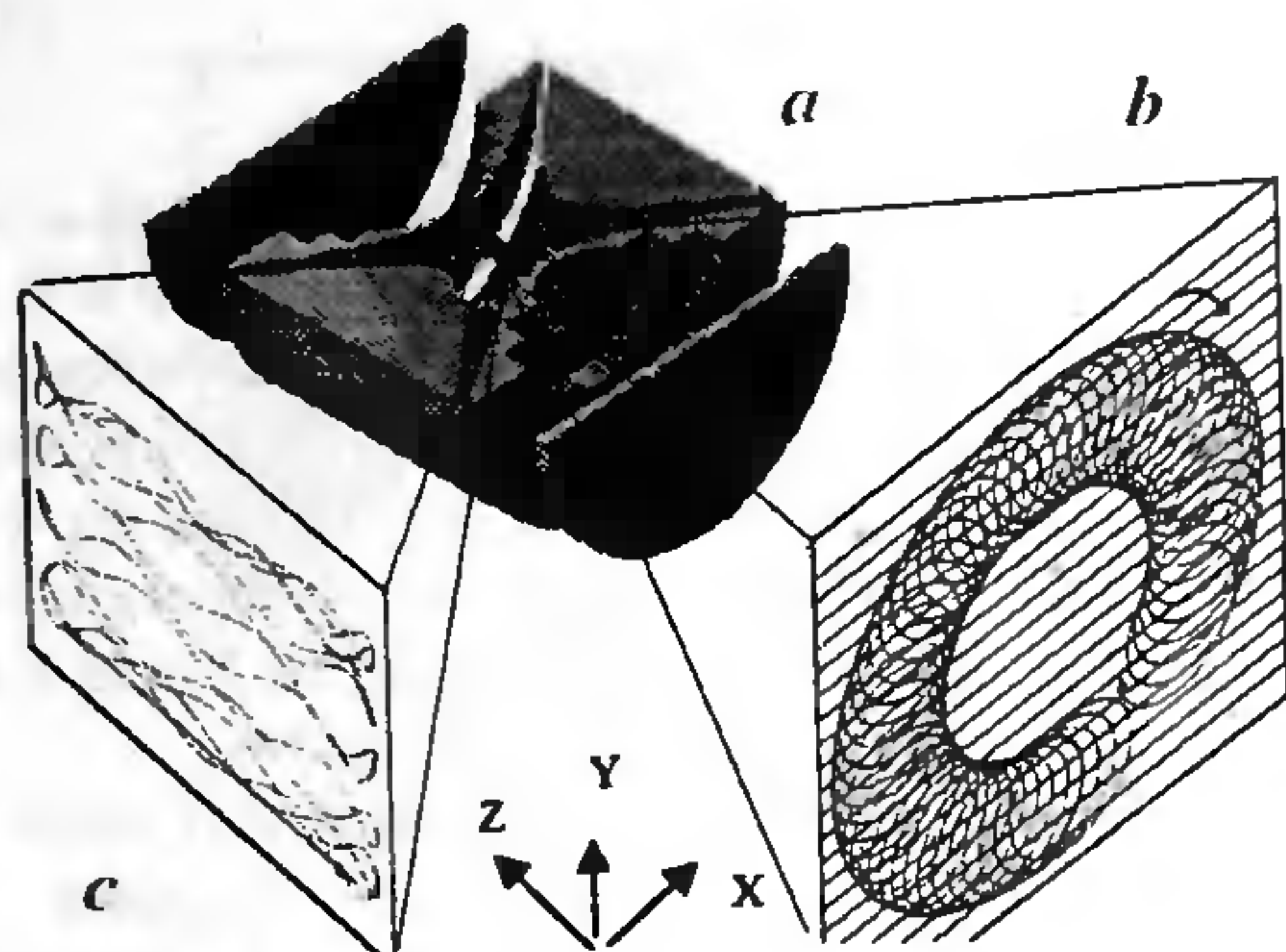


Figure 1. *a*, Trajectory of ions in a Penning trap; *b*, Motion as seen along the axial direction consists of high frequency cyclotron motion and the low frequency magnetron motion and *c*, The axial motion.

force exerted by the magnetic field. In the absence of this radial force the modified cyclotron frequency due to insertion of eq. (4) into eq. (2) is

$$m \frac{\omega^2}{r} = qB_0 \omega r - qE_0 r, \quad (5)$$

which is quadratic in ω . Solving for ω we get the expression for the two natural frequencies of oscillation of ion within the ion trap – the cyclotron (ω_c) and the magnetron frequency (ω_m) which are given by the expressions

$$\omega_c = (qB_0 + (q^2 B_0^2 - 4mqE_0)^{1/2}) / 2m, \quad (6a)$$

$$\omega_m = (qB_0 - (q^2 B_0^2 - 4mqE_0)^{1/2}) / 2m. \quad (6b)$$

While cyclotron motion is the predominant motion, eq. (6b) points to a second natural motion of the ion – the magnetron motion. The magnetron frequency is the precessional frequency of ion along a path of constant electrostatic potential. As can be seen by comparing eq. (6a) and (6b), the magnetron frequency is typically much smaller than the cyclotron frequency especially if E_0 is small.

In addition to two oscillations discussed above, the ions undergo one more oscillation referred to as the trapping oscillation, on account of the dc bias voltage applied to the two opposite electrodes perpendicular to magnetic field (Figure 1 *c*). These oscillations are in the axis parallel to the magnetic field (in the z -direction) and are also generally of a lower frequency compared to the cyclotron frequency. Assuming that the electrostatic potential between the two flat electrodes varies quadratically with distance (from the centre of the trap), the trapping oscillation (ω_z) has the form⁶

$$\omega_z = 2\pi\nu_z = 2\sqrt{qV_z/m}/d, \quad (7)$$

where d is related to the specific geometry of the trap, V_z is the applied dc bias potential on the two electrode and ν_z is the trapping frequency.

If the charged particle moves in a uniform magnetic field in such a manner that its velocity vector \vec{v} makes an angle α with the direction of the magnetic induction B , the path of the particle will be a helix of radius r and pitch h , where⁷

$$r = \frac{m v \sin \alpha}{q B} \text{ and } h = \frac{2\pi m v \cos \alpha}{q B}. \quad (8)$$

When a three-electrode trap geometry (similar to the Paul trap) is used, the angular frequencies of all three motions are modified to incorporate the trap geometry. The cyclotron frequency, axial frequency, magnetron frequency and the cyclotron frequency modified by the electric field (ω'_c) are now given by^{5,8,9}

$$\omega_c = \frac{qB}{m}, \quad (9a)$$

$$\omega_z = \left[\frac{4eV}{M(r_0^2 + 2z_0^2)} \right]^{1/2}, \quad (9b)$$

$$\omega_m = \frac{\omega_c}{2} - \left(\frac{\omega_c^2}{4} - \frac{\omega_z^2}{2} \right)^{1/2}, \quad (9c)$$

$$\omega'_c = \frac{\omega_c}{2} + \left(\frac{\omega_c^2}{4} - \frac{\omega_z^2}{2} \right)^{1/2}, \quad (9d)$$

where r_0 is the radius of the central ring electrode and $2z_0$ is the separation of the two end cap electrodes. The cyclotron frequency is related to the other frequencies of oscillation by the expression⁵

$$\omega_c^2 = \omega'^2_c + \omega_m^2 + \omega_z^2. \quad (10)$$

Linear trap and Paul trap

Motion of ions in the rf fields

The linear ion trap and the Paul trap are devices which use shaped electrodes and only *rf* oscillating fields (on which a dc potential may be superimposed for specific application) to trap ions. The stability of ions within the traps can be obtained by examining the force F_u experienced by a single ion of mass m , in the $u(x, y, z)$ direction, expressed as⁹⁻¹¹

$$F_u = m \frac{d^2 u}{dt^2} = -e \frac{d\phi}{dt}, \quad (11)$$

where ϕ is the effective potential in the trap between pairs of rods for the linear trap or between the ring and the end-cap electrodes in a three-dimensional Paul trap.

Solutions to this second-order linear differential equation are obtained by re-writing the equations of motion to fit the canonical form of the well-studied Mathieu equation¹²

$$\frac{d^2 u}{d\xi^2} + (a_u - q_u \cos 2\xi)u = 0, \quad (12)$$

where for the linear trap, ξ , a dimensionless parameter and the Mathieu parameters a_u and q_u are given by⁹

$$\xi = \omega_{rf} t / 2, \quad (13a)$$

$$a_u = a_x = -a_y = \frac{4eU}{m\omega_{rf}^2 r_0^2}, \quad (13b)$$

$$q_u = q_x = -q_y = \frac{2eV}{m\omega_{rf}^2 r_0^2}, \quad (13c)$$

and for the three-dimensional Paul trap these parameters are expressed as¹⁰

$$a_z = -2a_r = \frac{-8eU}{m\omega_{rf}^2 r_0^2}, \quad (14a)$$

$$q_z = -2q_r = \frac{-4eV}{m\omega_{rf}^2 r_0^2}, \quad (14b)$$

where ω_{rf} is the rf drive frequency. Stable region of ion trajectories (Figure 2), given as a plot of iso- β_u contours, are characterized by the values of a_u and q_u such that β_u is between 0 and 1. The values of β_u are computed from the continuing fraction¹¹

$$\beta_u^2 = a_u + \frac{q_u^2}{(\beta_u + 2)^2 - a_u - \frac{q_u^2}{(\beta_u + 4)^2 - a_u - \frac{q_u^2}{(\beta_u + 6)^2 - a_u - \dots}}} \quad (15a)$$

$$+ \frac{q_u^2}{(\beta_u - 2)^2 - a_u - \frac{q_u^2}{(\beta_u - 4)^2 - a_u - \frac{q_u^2}{(\beta_u - 6)^2 - a_u - \dots}}$$

which, to a first order approximation, can be written as

$$\beta_u^2 = a_u + \frac{q_u^2}{2}. \quad (15b)$$

The stability plot (Figure 2) indicates that all $a_u - q_u$ values lying outside the area bounded by $\beta_z = 0$ to 1 and $\beta_r = 0$ to 1 will have unstable trajectories. A choice of an $a_u - q_u$ can be translated to dc voltage (U) and rf amplitude (V) values by substitution in eq. (13) and eq. (14). Similarly, any point chosen within the stable region will provide stable trajectories at the computed U and V values, for a given mass m , frequency ω_{rf} and r_0 .

By way of a caution it must be noted that while the $(a_u - q_u)$ stability plot indicates regions of 'mathematical' stability, there are other factors which could cause ion loss. These include situations where ions, formed close to one of the electrodes (rather than at the centre), collide with the electrodes during oscillation. Further, ion-neutral and ion-ion interactions may lead to resultant charged species developing unstable trajectories because of the change in their q_u values.

Three characteristics of the ion cloud are used for different applications. First of these is the secular frequency of the ion in the specific trap. The second important factor is to know the potential well depth that will give an estimate of the energies required for destabilizing the ion from the trap. Finally, it may be instructive to know the space charge limits of the ion cloud. These three characteristics will next be discussed⁹.

Secular motion

Using the pseudopotential well approximation¹³, which assumes that the motion of the ion in an rf trap is composed of its secular motion and a micromotion due to the high frequency rf drive (Figure 3), it is possible to derive the equation governing the motion of the ions in the z -direction as^{9,13}

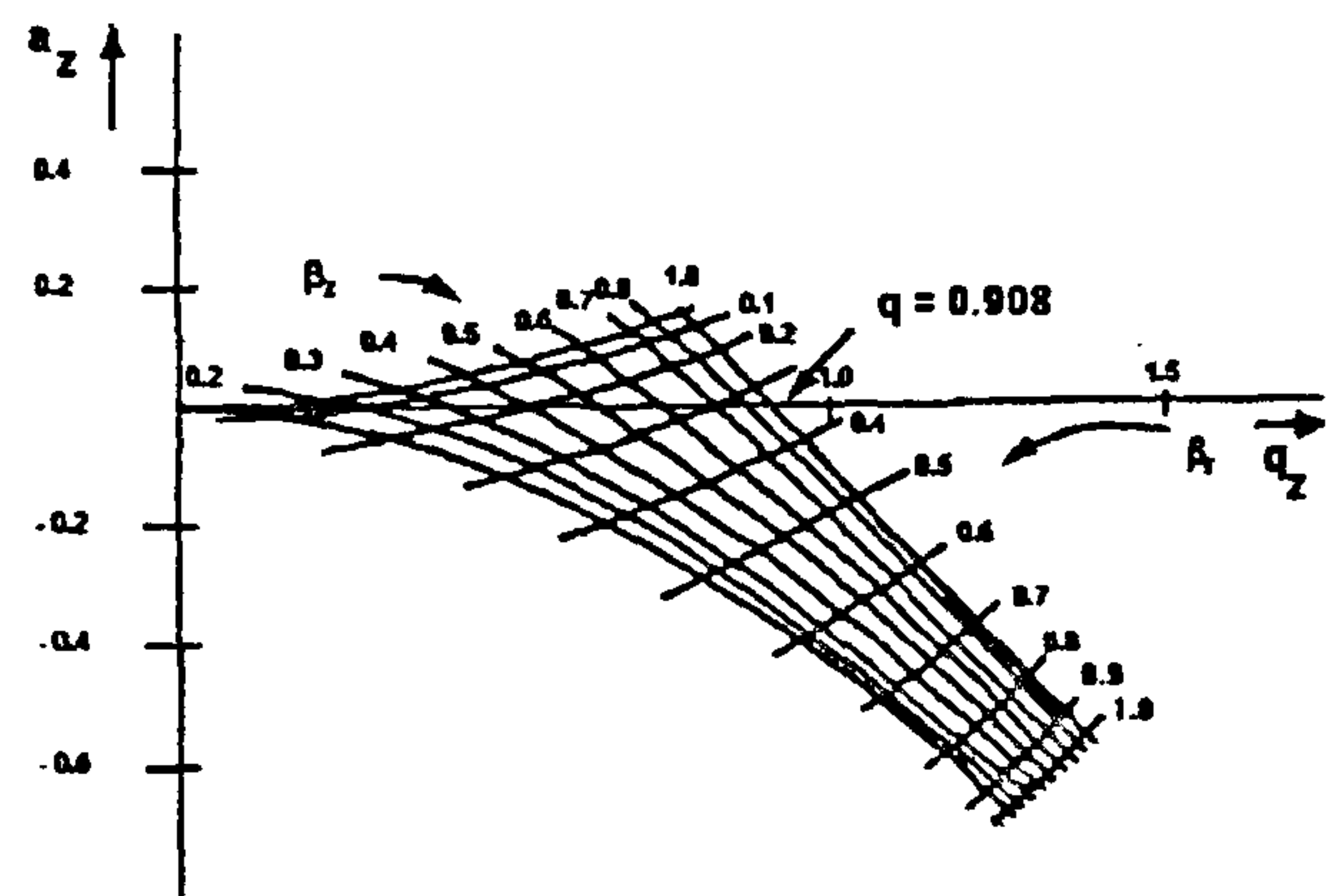


Figure 2. Mathieu stability plot for the Paul trap.

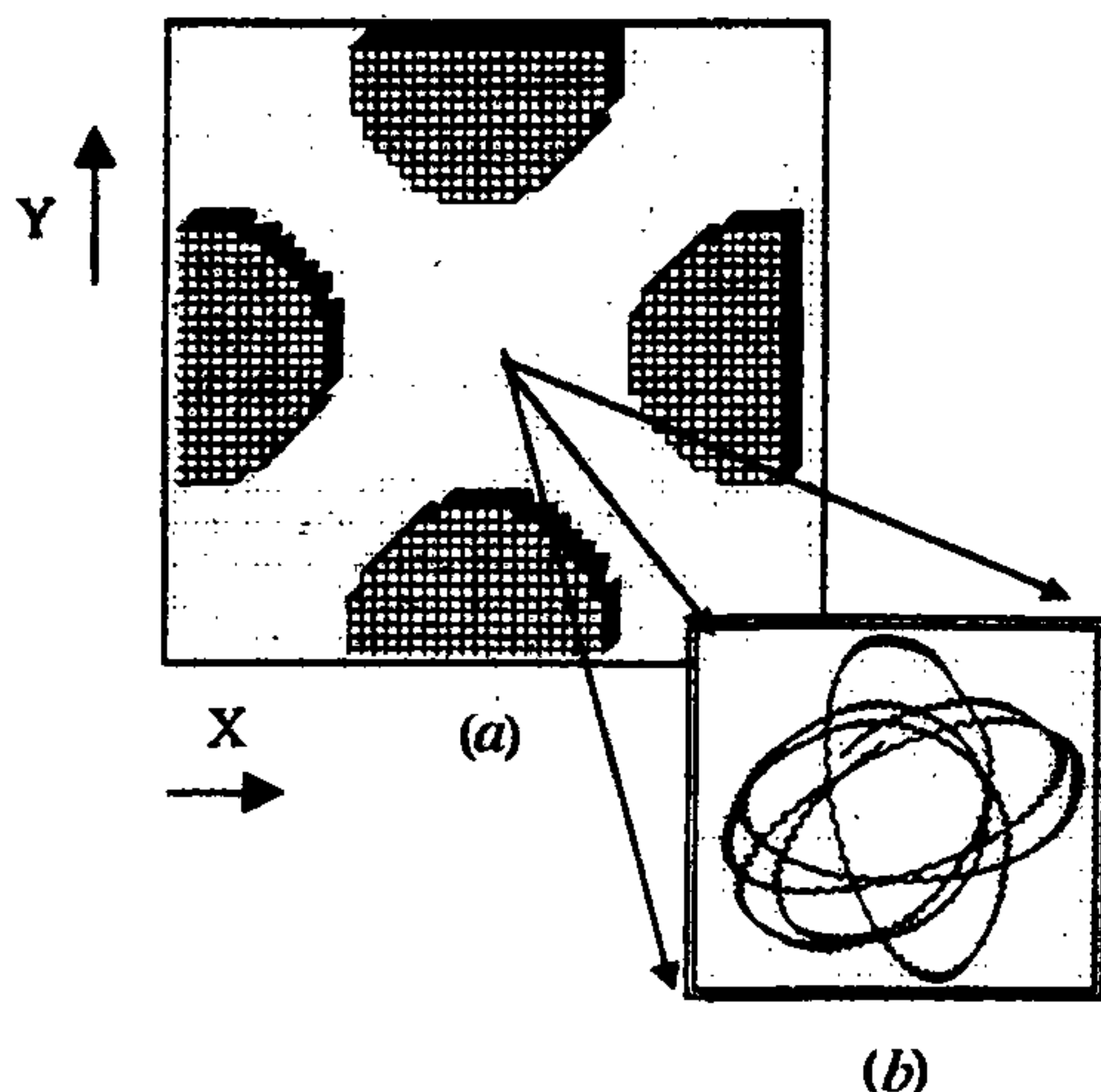


Figure 3. *a*, The cross-sectional view of the linear trap; *b*, The trapped ion undergoing a micromotion corresponding to the *rf* drive frequency ω_{rf} and a macromotion corresponding to the secular frequency $\omega_{secular}$.

$$\frac{d^2z}{dt^2} = \frac{\omega_{rf}^2}{4} \left(a_u + \frac{q_u^2}{2} \right) z. \quad (16)$$

When this is compared with the equation of simple harmonic motion, the secular frequency $\omega_{secular}$, may be written as

$$\omega_{secular} = \left(a_u + \frac{q_u^2}{2} \right)^{1/2} \frac{\omega_{rf}}{2}, \quad (17)$$

which gives

$$\omega_{secular} = \frac{\beta_u}{2} \omega_{rf} \quad (18)$$

with the approximation

$$\beta_u = \left(a_u + \frac{q_u^2}{2} \right)^{1/2}. \quad (19)$$

This approximation (eq. (19)) is referred to in literature as Dehmelt or adiabatic approximation¹¹. Since the secular frequency is related to β_u , which in turn is related to a_u and q_u , it is possible to compute the secular frequencies by inserting the experimental values in eqs (14a) and (15a).

Dehmelt potential

In accordance with the pseudopotential well approximation, assuming that $a_u = 0$, the force experienced by an

ion of mass m and charge e in terms of Dehmelt potential^{14,15} can be given by

$$m \frac{d^2z}{dt^2} = -e \frac{dD_z}{dz}, \quad (20)$$

from which for the linear trap we get

$$D_x = D_y = \frac{eV^2}{4mr_o^2\omega_{rf}^2}, \quad (21)$$

and for the 3D Paul trap gives

$$D_z = 2D_r = \frac{eV^2}{4mz_o^2\omega_{rf}^2}. \quad (22)$$

Eqs (21) and (22) relate the potential well depth of an ion of mass m trapped with a *rf* drive frequency, ω_{rf} , and a *rf* potential V . Figures 4 and 5 are SIMION¹⁶ simulation of trapping fields experienced by the ion. Figure 4 indicates the linear trapping field and Figure 5 shows the central low potential region to which all ions migrate to get trapped.

As an example, for the case of a linear trap, for a *rf* drive potential of $V = 100 V_{o-p}$, operating at a frequency of 1 MHz, the Dehmelt potential well depth D_z , experienced by ions between 20 and 200 amu varies as shown in Figure 6.

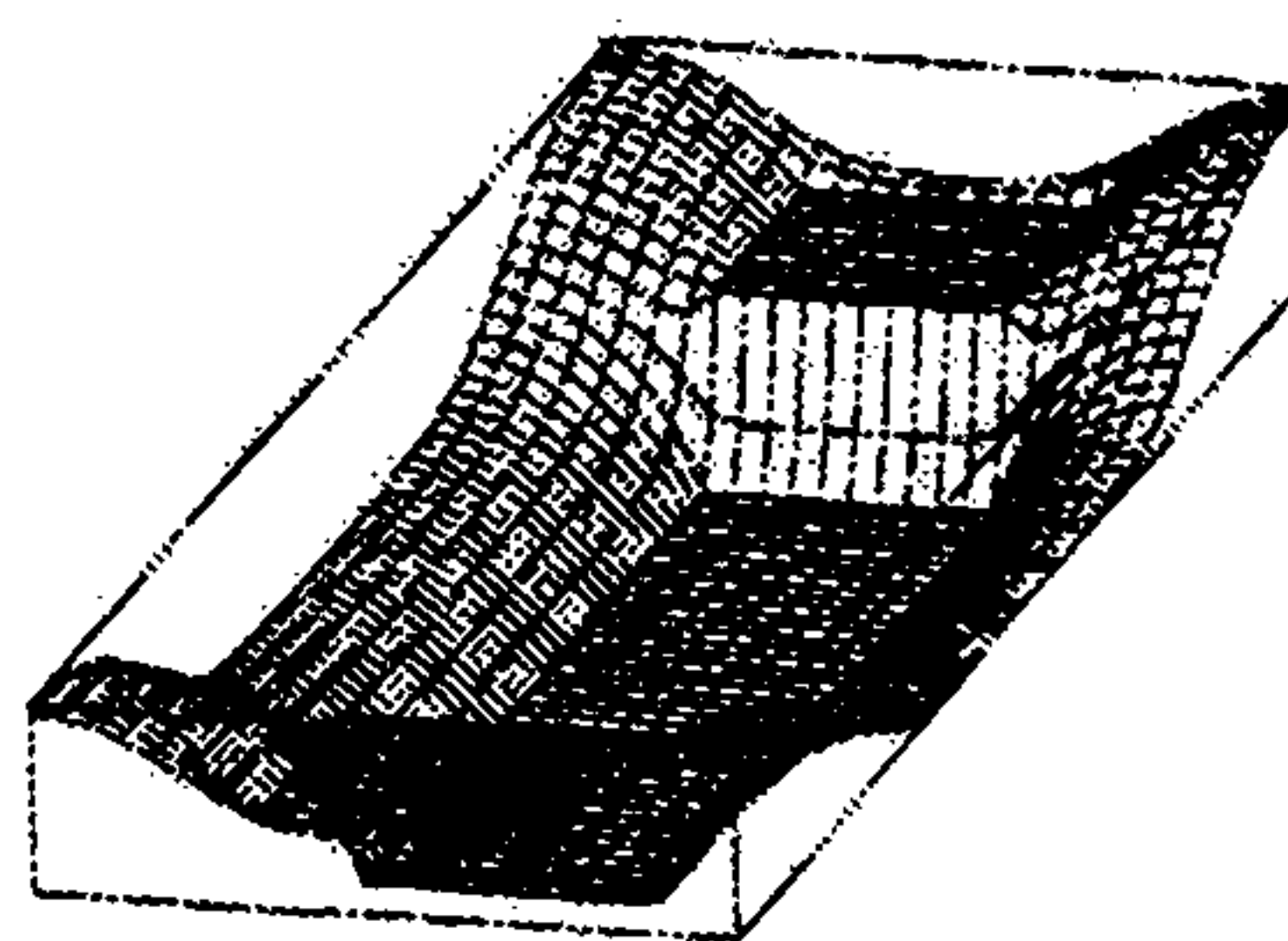


Figure 4. SIMION simulation of the potential well depth for a linear trap.

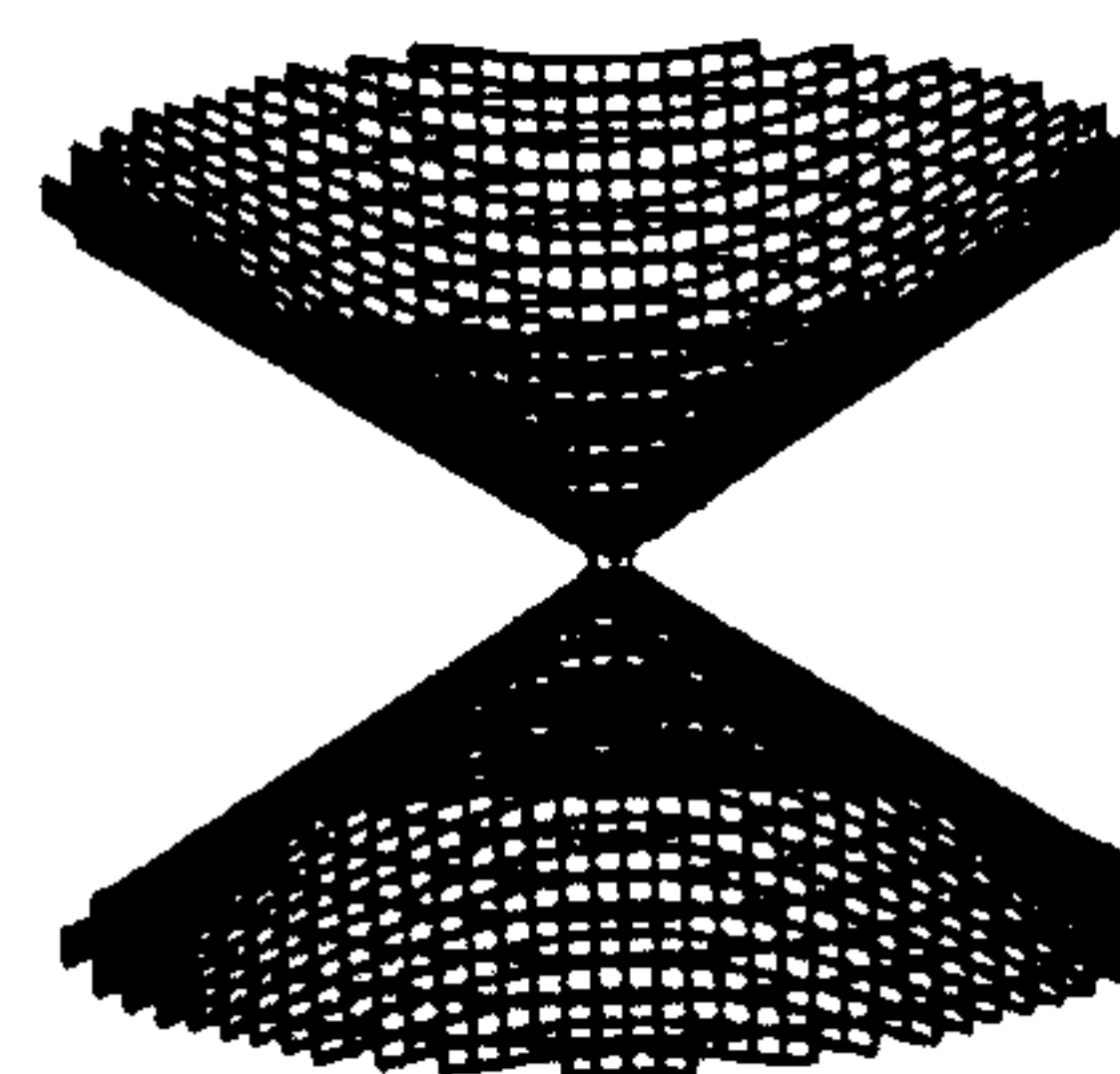


Figure 5. SIMION simulation of the potential distribution in a Paul trap.

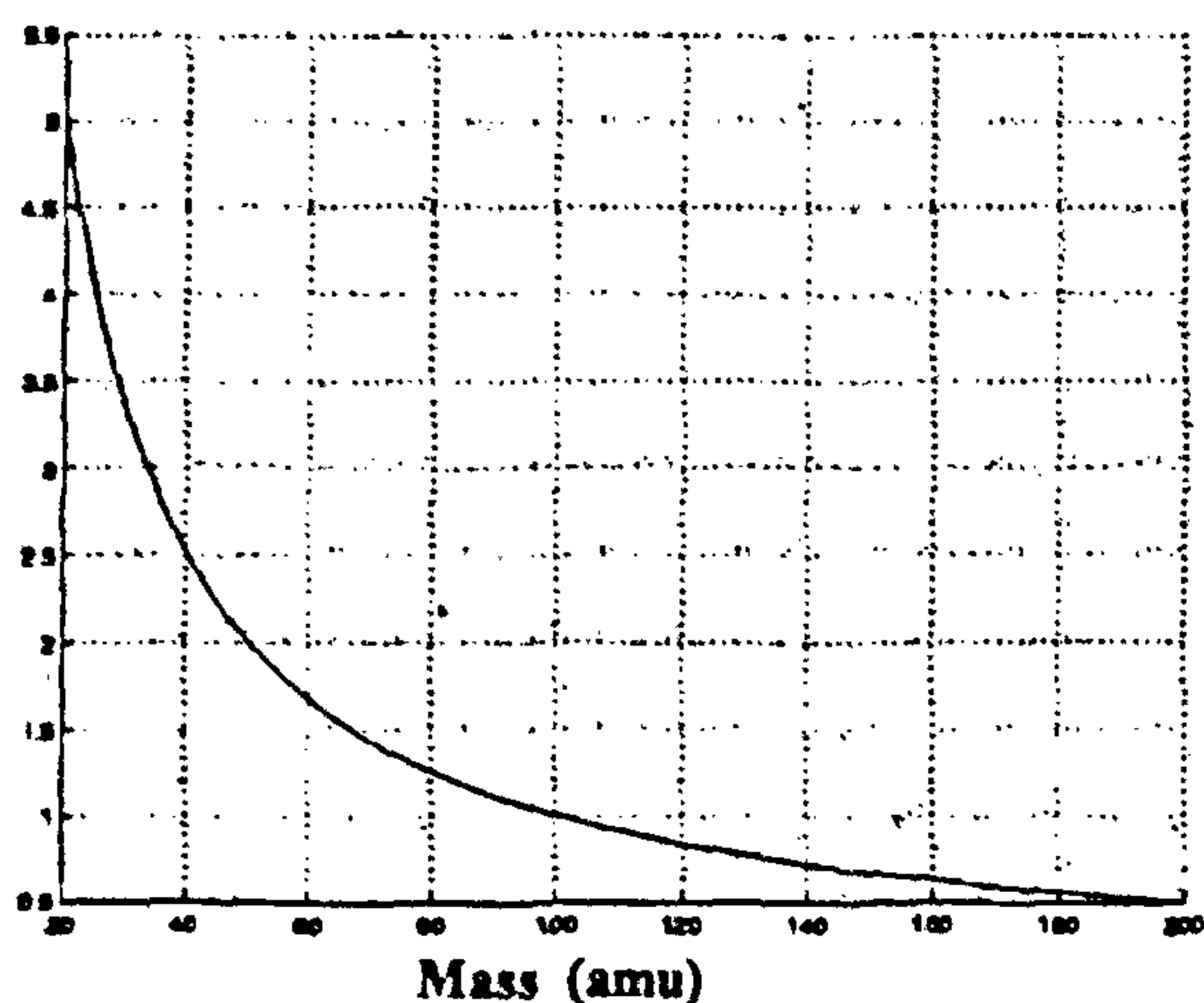


Figure 6. Variation of Dehmelt potential with mass for a linear trap.

Space charge limit

For a particle of charge Ze and mass m , moving in a two-dimensional quadrupole field ϕ , the space charge density may be computed using the Poisson's relation, $\nabla^2\phi = 4\pi\rho_{\max}$, the theoretical space charge density can be shown to be⁹

$$\rho_{\max} = \frac{D_x}{2\pi r_0^2} = \frac{eV^2}{8\pi m r_0^4 \omega_{\text{rf}}^2} \quad (23)$$

Hence the space charge N_{\max} ($=\rho_{\max}e$) for a linear trap expressed as

$$N_{\max} = \frac{D_x}{2\pi e r_0^2} = \frac{1}{2\pi e r_0^2} \left(\frac{eV^2}{4m r_0^2 \omega_{\text{rf}}^2} \right) = \frac{1}{32\pi} \frac{m\omega_{\text{rf}}^2}{e^2} q_z^2 \quad (24)$$

As an example, Figure 7 shows the variation of the space charge density N_{\max} with variation of the operating point q_z for two ions $^{138}\text{Ba}^+$ and $^{40}\text{Ar}^+$.

Similarly, the space charge limit computed for the Paul trap may be represented as

$$N_{\max} = \frac{3}{64} \frac{m\omega_{\text{rf}}^2}{e^2} q_z^2 \quad (25)$$

We will next turn on our attention to more practical aspects of trap construction and discuss parameters of importance in design of the several parameters involved. We have highlighted those that require special attention.

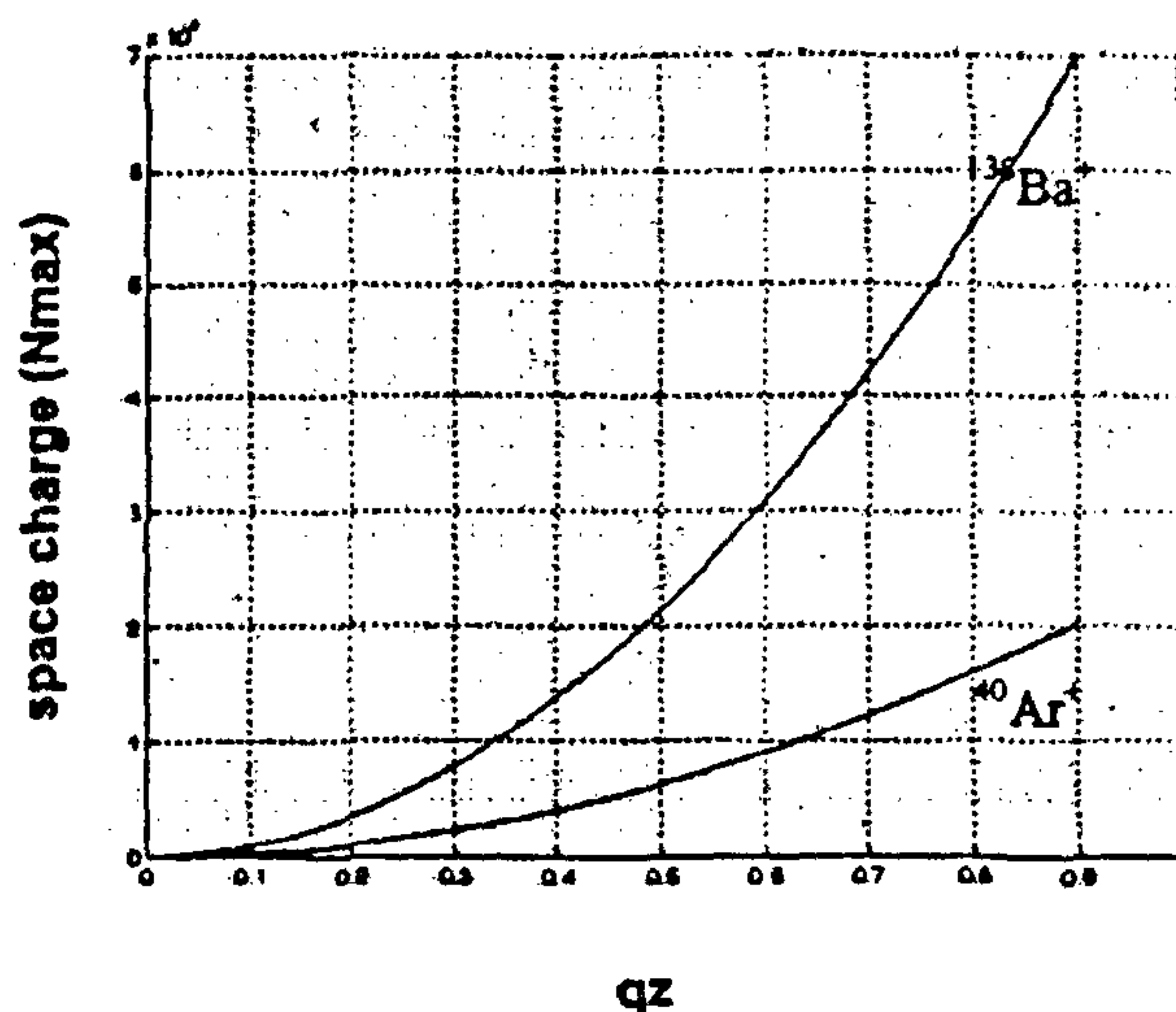


Figure 7. Variation of space charge with q_z for $^{138}\text{Ba}^+$ and $^{40}\text{Ar}^+$.

Design consideration

Penning trap

The trap consists of a three-electrode geometry mass analyser^{17,18} made of non-magnetic material which are shaped to conform to the eqs (26) and (27) (see below). This assembly is immersed in a high magnetic field superconducting magnet aligned with the z-axis of the trap parallel to the magnetic field. The two end cap electrodes are equally biased with low dc voltage with respect to the ring electrode for restricting ions in the axial motion.

There are several methods to detect the different frequencies of the ion motion in the Penning trap^{8,19,20}. These methods are different from conventional methods to measure low ion current and are rather subtle in that they measure the 'image current' developed across the end-cap electrode on account of the harmonic motion of the ions within the trap. In order to understand how this image current is generated, consider a simple two-electrode system within which an ion is undergoing circular motion (Figure 8).

As the ion traverses the path from one electrode to another, a small current is induced in both the electrodes. Similarly, when the ion traverses back, the direction of the induced current is reversed. While the magnitude of the induced current in the two electrodes remains the same, they are opposite phases. This causes an oscillating current, an 'image current', with frequencies matching the axial frequencies of the oscillating ions. It is this principle which is used for measuring ion currents and ion frequencies in Penning traps.

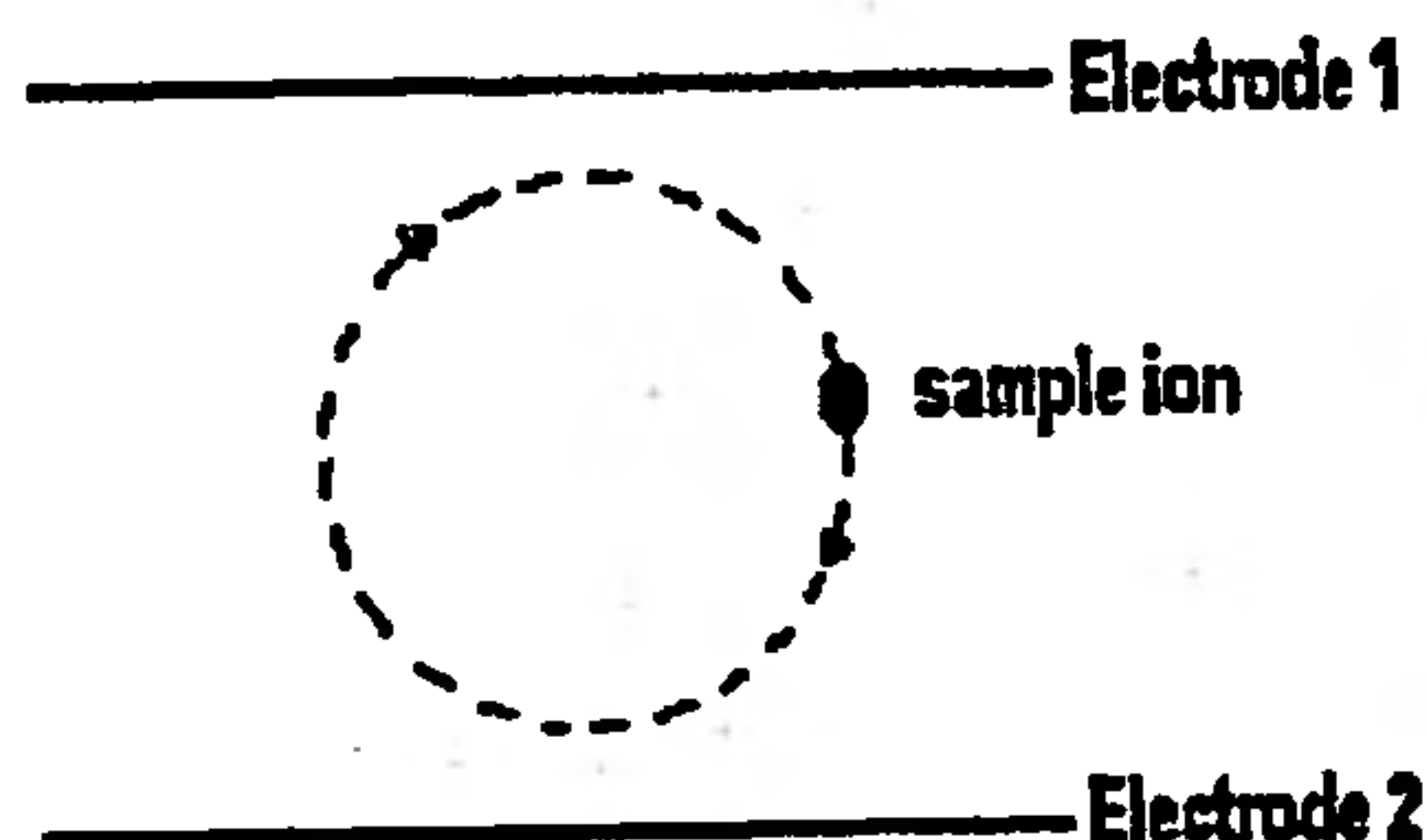


Figure 8. Circular motion of ions between the two electrodes.

The axial motion is detected by measuring the image current across the end cap electrodes⁸. The image current produced by the ions inside the trap are very small and in order to improve the signal strength, an external excitation signal is applied to the electrodes, so that more ions pick up the excitation and the image current with the excitation is easily detected at the excited frequency. In cases where a single or narrow band of frequencies are to be examined, the sensing resistor employs additionally a tuned tank circuit, to achieve a pure resistive sensing impedance, and avoid the time constants which would otherwise have a roll off at higher frequencies.

The cyclotron motion of a single ion has been detected and measured by various techniques. In one method²¹, where the central ring electrode is split into four isolated electrode quadrants, the image current detection is carried out by sampling the current across any two opposite pair of quadrants. A more recent technique¹⁹ involves the coupling of different modes by mode coupling of the required magnetron or cyclotron motion with that of the axial motion.

Linear trap

The linear trap is a device consisting of three segments^{21,22}, each segment being a four-rod assembly arranged as shown in Figure 9. In order to achieve the required quadrupolar field, the cross-section profile of the rods need to be hyperbolic. However, due to difficulties in machining such rods, a close approximation of the quadrupolar field may be achieved by using circular cross-section rods. The required trapping field is now obtained by maintaining $r/r_0 = 1.1468$, where r and r_0 are the radius of the cylindrical electrode and the radius of inscribed circle of the quadrupolar assembly^{9,23}.

From the point of view of trapping and isolating ions in linear traps, four factors are critical. These include: (1) geometric alignment and machining accuracy of the individual rods; (2) the need for the low initial energy of the ions introduced into the trap; (3) the requirement of high stability of all electronics circuits used; (4) the

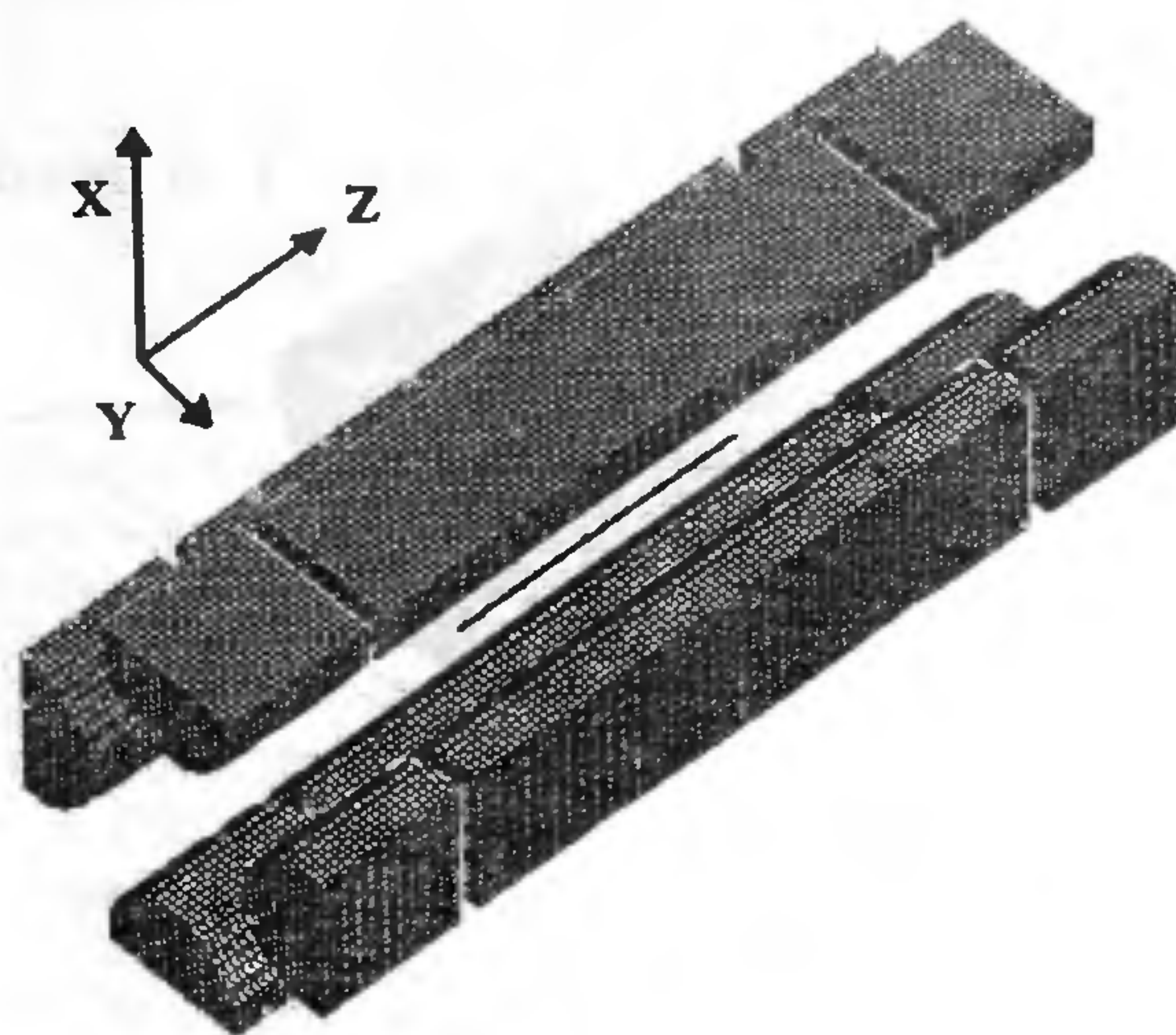


Figure 9. The three segment rod assembly of a linear trap.

electrical coupling of the three different segments which requires careful matching and tuning of the *rf* circuit.

Paul trap

The Paul trap consists of a 3-electrode geometry assembly with a hyperboloid of one sheet forming the central ring electrode and a hyperboloid of two sheets forming the two-end cap electrodes conforming to the following expression²⁴ (Figure 10)

$$\left(\frac{r^2}{r_0^2}\right) - \left(\frac{2z^2}{r_0^2}\right) = 1, \quad (26)$$

(ring electrode)

$$\left(\frac{r^2}{2z_0^2}\right) - \left(\frac{z^2}{z_0^2}\right) = -1, \quad (27)$$

(end-cap electrode)

where r_0 is the radius of the ring electrode and $2z_0$ is the axial separation of the end caps. These equations can be used to machine the ring and the end-cap electrodes after the choice of a suitable r_0 and z_0 is made.

For trapping ions in a Paul trap, *rf* excitation voltage is applied to the ring electrodes with no dc voltage when operating on the *q*-axis (i.e. $a_u = 0$ axis). The magnitude of the *rf* voltage applied has to be chosen for different experiments keeping in view the mass of ion to be trapped and the q_u value of the trapped ion (recall that q_u will determine the Dehmelt potential). Like the linear

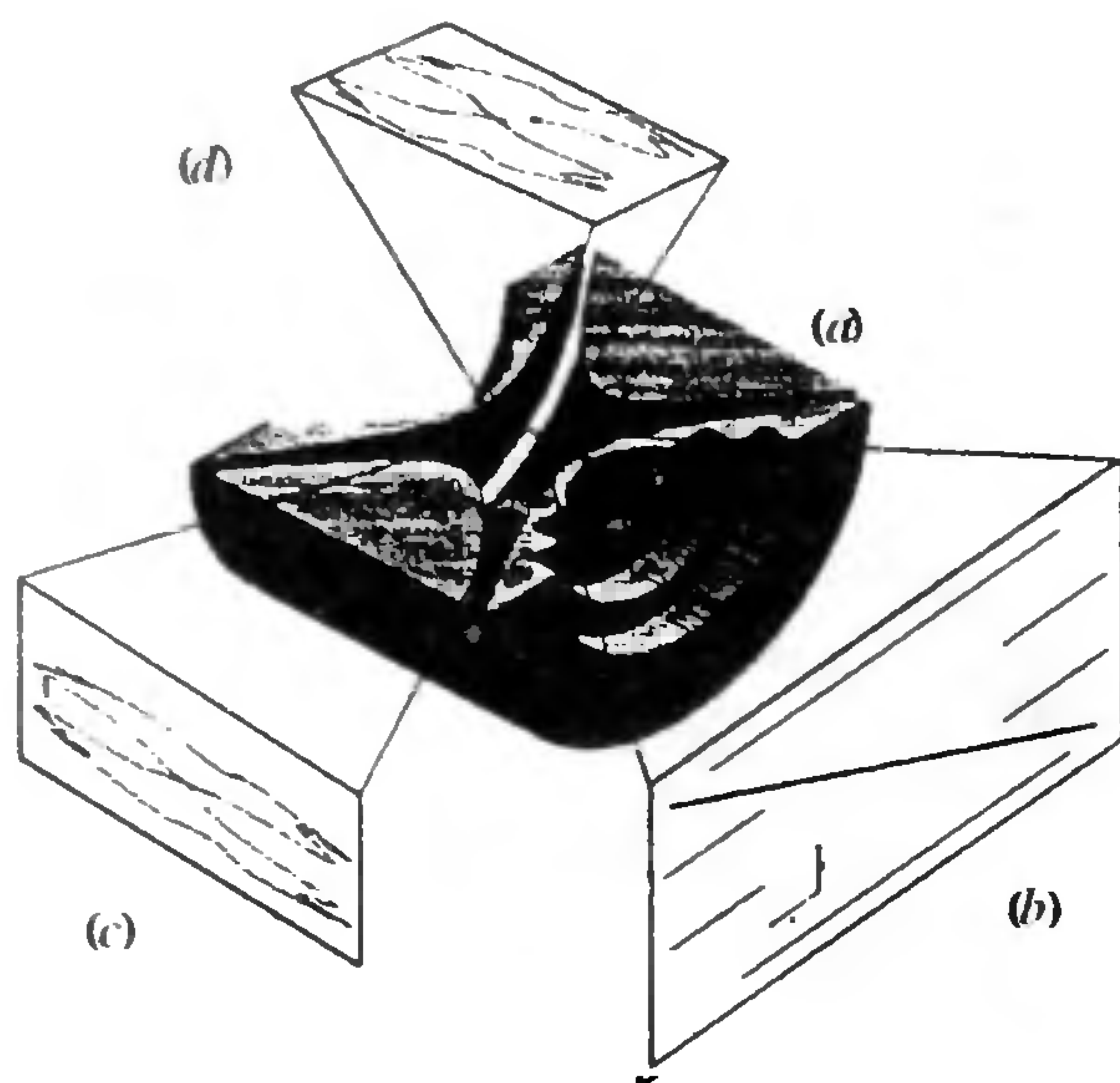


Figure 10. *a*, The Paul trap assembly crosssection showing the 3-electrode geometry; *b*, the motion of the sample ion as seen from the axial axis and *c*, *d* show the radial excursion of the trapped ion.

trap, dc potentials can also be superimposed on *rf* to operate at specific points on the stability plot.

Linear and Paul traps offer an attractive feature for isolation and trapping of targeted ions. It was shown that ions of different masses undergo secular motion in the *z*-axis (eq. (18)). The unwanted ions are ejected from the trap by applying an appropriate excitation with frequencies matching the secular frequencies of these ions. One of the common methods for generating this excitation signal is achieved by Stored Waveform Inverse Fourier Transform (SWIFT) technique⁶, where predetermined frequencies components are inverse Fourier transformed and synthesized in time domain, stored and applied when required in the experiment.

1. Penning, F. M., *Physica*, 1936, 3, 873.
2. Raizen, M. G., Gilligan, J. M., Bergquist, J. C., Itano, W. M. and Wineland, D. J., *J. Mod. Optics*, 1992, 39, 233–242.
3. Paul, W., *Rev. Mod. Phys.*, 1990, 62, 531–540.
4. Guan, S. and Marshall, A. G., *Int. J. Mass Spectrom. Ion Process.*, 1995, 146/147, 261–296.
5. Blatt, R., Gill, P. and Thompson, R. C., *J. Mod. Optics*, 1992, 39, 193–220.
6. Marshall, A. G. and Verdun, F. R., *Fourier Transforms in NMR, Optical and Mass Spectrometry*, Elsevier, New York, 1990.
7. Yavorsky, B. and Detaf, A., *Handbook of Physics*, Mir Publishers, Moscow, 1972, 537–539.
8. Brown, L. S. and Gabrielse, G., *Phys. Rev.*, 1986, A58, 223–311.
9. Dawson, P. H., *Quadrupole Mass Spectrometry and its Applications*, Elsevier, Amsterdam, 1974.
10. March, R. E. and Hughes, R. J., *Quadrupole Storage Mass Spectrometry*, Chemical Analysis Series 102, Wiley, New York, 1989.
11. March, R. E. and Todd, J. F. J., *Practical Aspects of Ion Trap Mass Spectrometry*, CRC Press, Florida, 1995, vol. 1.
12. MaLachlan, N. W., *Theory and Applications of Mathieu Functions*, Clarendon Press, Oxford, 1947.
13. Landau, L. D. and Lifshitz, E. M., *Mechanics*, Pergamon Press, Oxford, 1976, vol. 1.
14. Dehmelt, H. G., *Adv. At. Mol. Phys.*, 1967, 3, 53.
15. Major, F. G. and Dehmelt, H. G., *Phys. Rev.*, 1968, 170, 91.
16. Dahl, D. A., SIMION 3D Version 6.0, Proceedings of the ASMS Conference on Mass Spectrometry and Allied Topics, Atlanta, Georgia, 1995, vol. 43, p. 717.
17. Bollen, G., Becker, S., Kluge, H. J., Koenig, M., Moore, R. B., Otto, T., Rainbault-Hartmann, H., Savard, G. and Schweikhard, L., *Nucl. Instrum. Meth. A*, 1996, 368, 675–679.
18. Carlberg, C., Bergström, I., Bollen, G., Borgenstrand, H., Jertz, R., Kluge, H. J., Rouleau, G., Schwarz, T., Schwikhard, L., Senne, P. and Söderberg, F., *IEEE Trans. Instrum. Meas.*, 1995, 44, 553.
19. Cornell, E. A., Weisskoff, R. M., Boyce, K. R. and Pritchard, D. E., *Phys. Rev.*, 1990, A41, 312–315.
20. Weisskoff, R. M., Lafyatis, G. P., Boyce, K. R., Cornell, E. A., Flanagan, R. W. Jr. and Pritchard, D. E., *J. Appl. Phys.*, 1985, 63, 599–604.
21. Van Dyck, R. S. Jr., Scwinberg, P. B. and Delmelt, H., in *New Frontiers of High-Energy Physics* (eds Kursunoglu, B., Perlmutter, A. and Scott, L.), Plenum Press, New York, 1978.
22. Welling, M., Schuessler, H. A., Thompson, R. I. and Walther, H., *Int. J. Mass. Spectrom. Ion Process.*, 1998, 172, 95–114.
23. Dension, D. R., *J. Vac. Sci. Technol.*, 1971, 8, 266.
24. Knight, R. D., *Int. J. Mass Spectrom. Ion Process.*, 1983, 51, 127.